

# INTEGRATION OF ORBIT TRAJECTORIES IN THE PRESENCE OF MULTIPLE FULL GRAVITATIONAL FIELDS

**Matthew M. Berry<sup>\*</sup>**  
**Vincent T. Coppola<sup>†</sup>**

In this paper we demonstrate the effect of including multiple full gravitational fields in numerical orbit propagation, compared to only including one gravitational field and modeling the other bodies as point masses. Several test cases are examined in the Earth-Moon and the Jovian and Saturn systems. The tests show the increased accuracy gained by modeling multiple gravity fields. The tests also show the effect of changing the reference frame of the integration on the integrated trajectory.

## INTRODUCTION

High-fidelity orbit propagation and orbit determination require accurate force modeling. For some missions, particularly lunar and interplanetary missions, modeling third bodies as point masses may not be sufficient to meet accuracy requirements. Higher-order gravity field terms can be included; however, including these terms increases the runtime of the orbit propagation. A study showing the increase in accuracy that including multiple full gravitational fields provides is required so mission analysts can decide whether including multiple gravity fields is necessary to meet their accuracy requirements. In this paper, we present such studies, in the Earth-Moon system as well as in the Jovian and Saturnian systems.

In the first study, orbits around Earth at various altitudes are considered. The orbits are propagated once with the Moon's gravity modeled as a point mass, and then propagated using a lunar gravity field that includes J2 and higher terms. The ephemeris from the different propagations is compared to show the effect that the lunar gravity field has on the final position. The study is designed to show in which Earth orbit regimes the lunar gravitational field becomes significant.

A similar study is performed in lunar orbit. Lunar orbits at various altitudes are considered, propagated once with the Earth included as a point mass, and then propagated

---

<sup>\*</sup> Sr. Astrodynamics Engineer, Analytical Graphics, Inc. 220 Valley Creek Blvd. Exton, PA 19341.  
mberry@agi.com.

<sup>†</sup> Sr. Astrodynamics Specialist, Analytical Graphics, Inc. 220 Valley Creek Blvd. Exton, PA 19341.  
vcoppola@agi.com.

including the Earth's J2 and higher terms. The ephemeris produced by the propagations is compared to show the effect that Earth's gravity field has on lunar orbits.

A third study considers targeting a transfer orbit from the Earth to the Moon. This study compares solving for a transfer orbit with various combinations of the Earth and Moon gravitational fields included. The study shows the sensitivity of the solution to the transfer problem to the gravitational fields used. The study also examines the choice of reference frame for the transfer trajectory's propagation.

Similar studies are performed in the Saturnian system for orbits about Enceladus and in the Jovian system for orbits about Europa. Missions to these moons are currently being contemplated by NASA.

## EQUATIONS OF MOTION

The equations of motion for a spacecraft (Ref. 1) can be written

$$\ddot{\mathbf{r}} = -\mu \frac{\mathbf{r}}{\|\mathbf{r}\|^3} + \sum_{i>0} \mu_i \left( \frac{\mathbf{r}_{Bi} - \mathbf{r}}{\|\mathbf{r}_{Bi} - \mathbf{r}\|^3} - \frac{\mathbf{r}_{Bi}}{\|\mathbf{r}_{Bi}\|^3} \right) + \frac{1}{m} \mathbf{F}_S - \frac{1}{M_0} \mathbf{F}_0 \quad (1)$$

where

$B_i$	The $i$ -th gravitational body being modeled.
$B_0$	The reference gravitational body. Its location is the origin for the coordinate system.
$\mathbf{r}$	The position of the spacecraft relative to a coordinate system with origin $B_0$ and non-rotating axes (e.g., J2000 axes or ICRF axes).
$\ddot{\mathbf{r}}$	The acceleration of the spacecraft.
$\mathbf{r}_{Bi}$	The position of $B_i$ relative to $B_0$ .
$\mu$	The gravitational parameter for $B_0$ (i.e. $GM_{B_0}$ )
$\mu_i$	The gravitational parameter for $B_i$ (i.e. $GM_{B_i}$ )
$m$	The mass of the spacecraft.
$\mathbf{F}_S$	The sum of all forces on the spacecraft other than the point-mass gravitational force caused by all the celestial bodies (e.g., additional gravitational forces over the point-mass effect, drag, solar radiation pressure, general relativistic corrections, etc.).
$M_0$	The mass of $B_0$ (i.e. $M_{B_0}$ )
$\mathbf{F}_0$	The sum of all other forces on $B_0$ other than the point-mass gravity of the other celestial bodies.

The first term in (1) is the point-mass effect of gravity of  $B_0$  on the spacecraft and the second term is the third-body gravity perturbation acceleration arising from the point-mass gravitational effects of the other celestial bodies. The indirect terms of the third-body accelerations and the force  $\mathbf{F}_0$  arise from the non-inertial nature of the coordinate

system used to express the equations of motion. These terms would not appear if the origin for the coordinate system were taken to be an inertial point, e.g. the solar system barycenter.

Note that the motions of the celestial bodies are taken to be known as a function of time – the motion of the spacecraft and bodies are not being solved simultaneously. The most precise ephemerides for planets and moons are available from JPL. JPL’s Developmental Ephemeris 418 (Ref. 2), available as of Jan 2008, was derived from a numerical integration of the Sun, the planets (using barycenter values for the outer planets), and the Earth’s Moon. The equations of motion considered general relativistic effects, oblateness of the Earth, and certain other effects. The ephemerides were further refined using planetary and lunar laser ranging observations. Thus, the motion of the bodies is not simply driven by point-mass gravity.

Ephemerides for the moons of other planets are also available from JPL, in SPICE format (Ref. 3), created by investigators using the best knowledge of the force environment at the time. Currently, the best ephemerides for the Mars, Saturn, Uranus, and Pluto systems are based upon the DE414 ephemerides (succeeded by the DE418), while the Jupiter and Neptune systems are based upon DE405. System ephemerides were numerically integrated using point-mass gravitational effects, perturbations arising from the oblateness of the primary planet, and relativistic perturbations and then fit using mission observations (as available). A discussion of the Saturnian system is given in Ref. 4 and the Jovian system in Ref. 5.

As of this writing, there are no consistently based ephemerides for the entire solar system available from JPL (i.e. no set of SPICE files containing the planets, barycenters and moons all referenced to the same DE ephemerides). Moreover, no system ephemerides have been recomputed for the updated DE418. Because DE418 contains updates to the ephemeris of Mars, Earth, the Moon, and (most significantly) Saturn, we wanted to use it in our studies. Therefore, for these studies, we created a set of ephemerides for the solar system based upon DE418 by selectively extracting barycenter, planet center, and moon ephemerides from the currently available set of SPICE files. This was done using SPICE software utilities available from JPL (Ref. 3).

## **Gravitational Fields**

The effects of the gravity fields of the celestial bodies, apart from the point-mass effect, appear in two ways. Each gravitational field produces a force on the spacecraft as part of  $\mathbf{F}_S$ ; this is a direct term computed by evaluating the gravity field at the position of the spacecraft. The gravitational field, however, also produces a force on the reference body  $B_0$  as part of  $\mathbf{F}_0$  (excepting of course the field of  $B_0$  itself); this is an indirect term computed by evaluating the gravity field of  $B_i$  at the location of  $B_0$ . Looking at (1), one can see that the third-body gravitational fields (i.e., the fields other than that of the primary body  $B_0$ ) appear in the equations of motion as a tidal term just as the point-mass part of the fields do:

$$\mathbf{g}_{B_i}(\mathbf{r} - \mathbf{r}_{B_i}) - \mathbf{g}_{B_i}(-\mathbf{r}_{B_i}) \quad (2)$$

where  $\mathbf{g}_{B_i}(\boldsymbol{\rho})$  denotes the acceleration produced by the gravitational field of body  $B_i$  at a location  $\boldsymbol{\rho}$  from  $B_i$ .

When modeling the motion of a spacecraft within a planetary system, only those bodies that significantly contribute to the spacecraft acceleration need be included. Bodies outside of the system will contribute, if at all, only through point-mass gravity---the rest of the field can safely be ignored. Bodies within the system, however, are another matter. In many systems, e.g. the Jupiter and Saturn systems, the effects of planetary oblateness are significant enough that they must be included when determining the ephemerides of the moons of the system. Spacecraft operating near these moons will be significantly perturbed by the moon's field and as well as the planetary field.

### **Choice of Reference Body**

In principle, the trajectory produced by solving (1) will be independent of the choice of reference body  $B_0$ . In practice, however, this may not be the case because of incomplete knowledge of the forces in  $\mathbf{F}_0$  and the sensitivity of the solution to the inclusion of certain forces. The results section shows that the sensitivity of the results to mismodeling is reduced when the mismodeling appears in (1) as a tidal term, rather than only a direct term.

Consider the case of a spacecraft operating near a planet's moon, where the moon's gravity field should be included in the modeling. If the moon's own ephemeris was computed using the planet's gravity field, then that field should be modeled on the spacecraft as well---if the gravity field is significant for modeling the moon, then it must be significant for bodies near that moon. If the planet is chosen as the reference body, the planet's gravity appears as a direct term in (1). If the moon is chosen as the reference, then the effect of the planetary field appears in (1) as a tidal term, that is, in the form of the difference in planetary gravitational acceleration at the spacecraft and moon locations.

There is an important difference between a direct and tidal term. If a direct term is neglected, the magnitude of the effect is taken as zero. If a tidal term is neglected, however, it is only the difference in the magnitude of the effect (evaluated at the spacecraft and at the reference body locations) that is zero, not the magnitude of the effect itself. Thus, higher order terms in a planetary gravitational field that must be included when using the planet as the reference body may be able to be safely neglected when using the moon as the reference body, when the spacecraft is orbiting the moon.

## **RESULTS**

### **Earth-Moon System**

To measure the effect of the lunar gravity field on an Earth-orbiting satellite, a study is performed comparing ephemeris generated with and without the lunar field. Ephemeris

is generated for eight satellites with periods between 1.5 hours and 120 hours. All of the satellites have zero eccentricity and zero inclination. Each orbit is propagated once with using a 24x24 EGM96 field (Ref. 6), the Moon as a point mass using the LP150Q gravitational parameter (Ref. 7), and the Sun as a point mass. The orbit is then propagated using the same settings for the Earth and Sun gravity, but with a 4x4 LP150Q lunar gravity field. In both cases the orbits are integrated with an eighth-order Runge-Kutta integrator using a constant 60-second step size. The ephemeris is generated over 30 days.

Figure 1 shows the position differences, in millimeters, between the orbits generated with and without the lunar geopotential terms. The differences shown are the maximum differences over the 30-day propagation. The figure shows the position differences increase with period, with periods less than 12 hours having less than a 1 mm difference over 30 days. For a geostationary orbit the difference is 5 mm, and the differences then increase quadratically. However, even with a 5-day orbit the difference is only 100 mm over 30 days, which is negligible for this type of orbit.

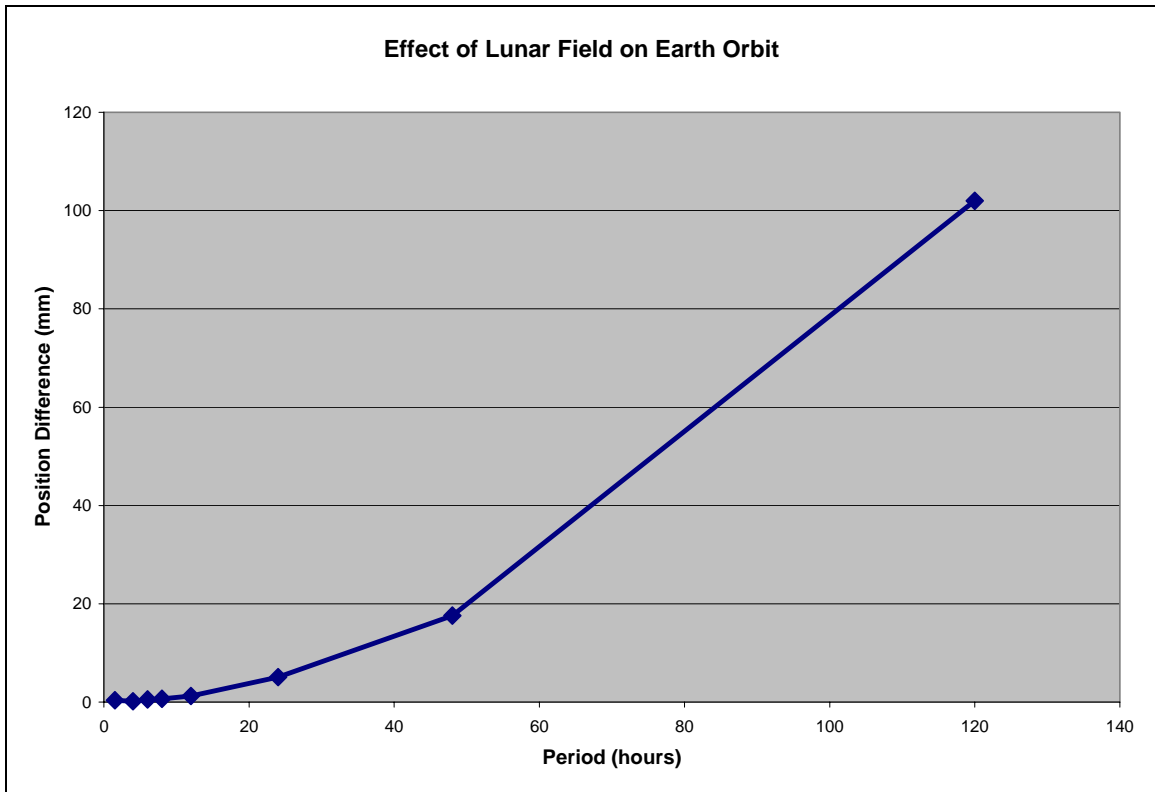


**Figure 1: Position difference between using 0x0 and 4x4 lunar fields**

To show the effect of the Earth’s gravity field on lunar orbits, a similar study is performed about the Moon. Ephemeris is generated for six satellites in lunar orbit with altitudes between 100 and 20,000 km. The initial conditions for each orbit are again zero eccentricity and zero inclination, and the orbits are generated for 30 days with a constant 60 second step. The orbits are generated once with a 70x70 LP150Q lunar gravity field,

the Earth as a point mass with the EGM96 gravitational parameter, and the Sun as a point mass. The orbits are then generated with the same settings for the Moon and Sun but with a 4x4 EGM96 field for the Earth.

Figure 2 shows the maximum position differences in meters over 30 days with and without the Earth’s geopotential terms, as a function of lunar altitude. Again, the figure shows a quadratic increase in the position difference as altitude increases, going from a 60 mm difference at 100 km, to 44 meters at 20,000 km altitude. These differences are more significant than the difference due to the lunar field in Earth’s orbit, but for most applications are most likely negligible over this propagation span.

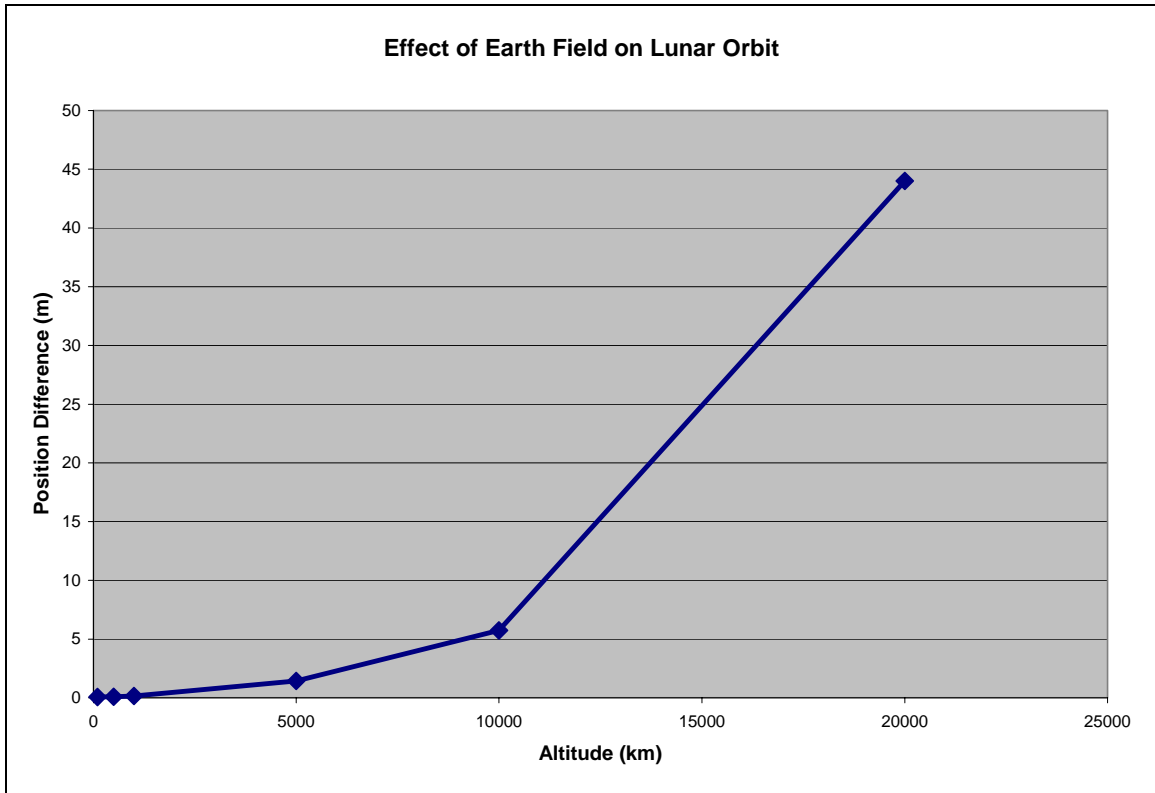


**Figure 2: Position difference between using 0x0 and 4x4 Earth field**

To show the effect of multiple fields on transfer trajectories from the Earth to the Moon, a study is performed to determine how the gravity field affects the maneuver needed to get into trans-lunar orbit. A typical Earth-to-Moon transfer orbit is modeled in STK/Astrogator maneuver planning software, which includes a differential corrector to solve for certain parameters. By varying the number of terms in each gravity field and comparing the solution given by the differential corrector, we can see the sensitivity of the solution to the fields.

A targeting sequence in STK/Astrogator is set up that starts in low-earth orbit, performs an impulsive maneuver (delta-V) in the velocity direction, and then propagates to lunar periapsis. The initial orbit is circular with a semi-major axis of 6678.136 km and an

inclination of 28.5°. The initial epoch is 1 Jul 2007 12:00:00 UTC. The propagation to lunar periapsis is performed with an eighth-order Runge-Kutta-Fehlberg integrator with seventh-order step size control. The integrator uses a relative tolerance of 1e-15, and an absolute tolerance of 1e-12.

The differential corrector is used on this targeting sequence to solve for the initial right ascension of the ascending node (RAAN), the initial true anomaly, and the delta-V magnitude needed to achieve a final lunar altitude of 100 km, a final lunar inclination of 90°, and a time of flight of five days. The differential corrector is run using different degrees and orders of the Earth and Moon’s gravitational fields during the propagation, and the solutions are compared. In all cases the EGM96 field is used for the Earth, the LP150Q field is used for the Moon, and the Sun is modeled as a point mass. No other forces are considered. The differential corrector is run with the Earth used as the reference body in the propagation in certain test cases, and with the Moon used as the reference body in other cases.

Table 1 shows the solutions found by the differential corrector for various combinations of Earth and Moon gravitational field terms when the Earth is used as the reference body for the propagation. The table shows that the Earth J2 term has a noticeable effect on the solution, changing the required delta-V by 3 m/s, the required RAAN by 0.05°, and the required true anomaly by 0.1°. While further increasing the number of terms does not significantly affect the required delta-V magnitude, it does have an effect on the RAAN and true anomaly. Increasing to a 4x4 Earth field changes the required RAAN by 0.0007° and the required true anomaly by 0.001° compared to using J2 only. The 0.001° change in true anomaly for this orbit effectively changes the start time of the maneuver by 15 milliseconds. Further increasing the field to 8x8 has a 2e-5° effect on true anomaly, which equates to less than one microsecond. The table shows that adding terms to the lunar gravitational field does not significantly affect the solution.

**Table 1: Solution to Earth-to-Moon transfer using Earth as the reference body**

Test case	Delta V (km/sec)	RAAN (deg)	True Anomaly (deg)
Earth 0x0 Moon 0x0	3.104443437	182.951386459	356.000696037
Earth 2x0 Moon 0x0	3.107154833	183.010315900	355.902066721
Earth 4x4 Moon 0x0	3.107104997	183.010994753	355.901351228
Earth 8x8 Moon 0x0	3.107087534	183.011126352	355.901375779
Earth 12x12 Moon 0x0	3.107084597	183.011172491	355.901368707
Earth 8x8 Moon 2x0	3.107087535	183.011172468	355.901334059
Earth 8x8 Moon 12x12	3.107087533	183.011170339	355.901333203

Table 2 shows the solutions found when the Moon is used as the reference body. Again, the solutions seem to converge once a 4x4 Earth field is used. Comparing Table 1 to Table 2 when using a 4x4 Earth field shows that the choice of reference body does not significantly affect the solution.

**Table 2: Solution to Earth-to-Moon transfer using the Moon as the reference body**

Test case	Delta V (km/sec)	RAAN (deg)	True Anomaly (deg)
Earth 0x0 Moon 0x0	3.104443431	182.951372880	356.000713593
Earth 2x0 Moon 0x0	3.107154818	183.010324652	355.902060432
Earth 4x4 Moon 0x0	3.107104983	183.011003507	355.901344938
Earth 8x8 Moon 0x0	3.107087519	183.011135106	355.901369489
Earth 8x8 Moon 2x0	3.107087521	183.011181225	355.901327763

Though Tables 1 and 2 don't show much sensitivity in the solution to gravity field terms beyond the Earth's 4x4 terms, the final position does vary with a different field. For instance, the difference between the final position with the 8x8 field and with the 4x4 field is 121 meters. While this position difference may be significant, the test shows that this difference, due to the choice of force model, is within the bounds of the maneuver uncertainty. So during maneuver planning, using the higher order field is unnecessary. However, after the maneuver is performed, and a post-maneuver orbit determination solution is found, higher order fields should be used to predict the actual lunar orbit insertion point.

### Enceladus

Enceladus is the second closest major moon of Saturn and travels in a nearly circular orbit. Cassini has discovered water there that may be in liquid form, erupting from the surface like geysers. Enceladus is being considered a possible destination for a mission, the Enceladus Explorer mission, with earliest launch date of 2020 (Ref. 8). The major moons of Saturn are listed below in Table 3.

**Table 3: Major moon in Saturn system**

Name	Number	Mass (1/Saturn)	Distance (Saturn radii)	Comments
Mimas	I	8.0e-08	3.08	Circular; Planar with Enceladus
Enceladus	II	1.3e-07	3.96	Circular
Tethys	III	1.3e-06	4.89	Circular; Planar with Enceladus
Dione	IV	1.8e-06	6.26	Circular; Planar with Enceladus; 2:1 resonance with Enceladus
Rhea	V	4.4e-06	8.74	Circular; Planar with Enceladus
Titan	VI	2.4e-04	20.27	Circular; Planar with Enceladus
Hyperion	VII	3.0e-08	24.60	Eccentric; Planar with Enceladus
Iapetus	VIII	3.3e-06	59.09	Eccentric; Inclined
Phoebe	IX	7.0e-10	214.91	Eccentric; Inclined

The first 5 moons constitute an inner system, the next 2 a middle system, and last 2 an outer system. Significant third-body gravity effects on Enceladus arise from Saturn, the other members of the inner system, and Titan (because of its mass). Iapetus is too far

away to have much influence. Numerical studies confirm that the third body gravity perturbations from Hyperion, Iapetus, and Phoebe can be ignored for this study.

We consider a nominally Enceladus orbiting trajectory, with initially zero eccentricity,  $60^\circ$  inclination with respect to the Enceladus orbital plane, and located at about 1.587 Enceladus radii (400 km from moon center, about 148 km above its surface). We arbitrarily choose the initial epoch as 1 Jul 2025 12:00:00. The gravity perturbation of Saturn is so strong that this trajectory eventually hits the surface in just over 3 days. Initial conditions with smaller altitudes impact in even short durations; those with radii above 2.54 leave the moon’s environment within a day (if they can avoid impact).

First, we compare numerically integrated trajectories using Enceladus as the reference body. The reference trajectory, for comparison purposes, includes the effects of the Enceladus gravity field (a 2x0 zonal field), Saturn’s gravity field (an 8x0 zonal field), and the third-body point mass effects of all other major moons, the Sun, and the Jovian system. All gravitational parameter values and gravity zonals for the celestial bodies were set from values indicated in the comments section of the SPICE files containing the ephemerides. This is consistent with the force modeling used to generate the ephemerides of the Saturn system (see Ref. 4) except that general relativistic effects are ignored. The maximum difference between the trajectories being studied and the reference, for a 3-day propagation, is shown below in Table 4.

**Table 4: Maximum difference against 8x0 Saturn field, using Enceladus reference frame**

Saturn’s gravity field	Maximum difference (m)
6x0	0.003
4x0	0.317
2x0	32.3
Point mass	4,050

Next we repeat the comparison, using Saturn as the reference body. The reference trajectory is computed using the same force modeling used for the previous reference trajectory, but is computed in the Saturn-referenced frame. When Saturn’s field includes only the point-mass effect, the trajectory impacts Enceladus in a little over 11 hours, so the maximum difference is computed over the shorter time interval for that case. The maximum differences are shown below in Table 5:

**Table 5: Maximum difference against 8x0 Saturn field, using Saturn reference frame**

Saturn’s gravity field	Maximum difference (m)
6x0	36.3
4x0	125
2x0	18,300
Point mass*	608,000

It is clear that the higher zonals do contribute to the ephemeris for this trajectory, even over this short duration. The Saturn-referenced results, however, are much more sensitive to the inclusion of particular zonals. At the distance of Enceladus, the J2, J4, J6, and J8 terms cause significant gravitational perturbations, so ignoring these terms produces large differences. In the case of the Enceladus-referenced system, Saturn's field appears in the equations only as a tidal term (i.e., in the form of the difference between the field evaluated at the spacecraft and the field evaluated at Enceladus) and since the spacecraft and Enceladus are close, the field's effect is much smaller.

Finally, we compare the choice of reference body in generating the trajectory in Table 6.

**Table 6: Maximum difference between Saturn and Enceladus reference frames**

Saturn's gravity field	Maximum difference (m)
8x0	2,130
6x0	2,110
4x0	2,070
2x0	19,100
Point mass*	608,000

The point mass comparison can only be performed for a propagation of just over 11 hours, as the Saturn-referenced trajectory impacts then.

The point-mass case shows a difference of 608 km from changing the reference body. With Saturn as the reference body, the point-mass case completely ignores the zonals, a large mismodeling error. In the Enceladus-referenced case, ignoring a zonal effectively means that Saturn's field is being modeled as if it has the same effect on the spacecraft as it does on Enceladus (i.e, the tidal term is precisely zero). So, while both point-mass propagations mismodel the field, the mismodeling appears in different ways in (1), with the appearance in tidal form generating a much smaller error. This result strongly suggests the use of the moon as the reference body when orbiting it.

The 2 km difference that occurs when using different reference bodies, even when using Saturn's full field, is again a mismodeling issue. This difference indicates that the full force field being considered is still inadequate. In fact, if we attempt to generate the trajectory of Enceladus itself using Saturn as the reference body, with an initial condition from the SPICE ephemeris, we find that the generated Enceladus trajectory differs from that provided by SPICE by 1.76 km over 3 days. Evidently, other forces must be included when integrating with Saturn as the reference. This result also suggests the use of the moon as the reference body when orbiting it, because any mismodeled force (apart from the moon's gravity) appears only as a tidal term in the equations of motion.

## Europa

Europa is the second closest major moon of Jupiter. The Europa Geophysical Explorer Mission is a proposed mission to do studies to locate liquid water and ice on Europa, with

earliest launch date of 2015 (Ref. 8). The major moons of Jupiter are listed below in Table 7.

**Table 7: Major moons in Jovian system**

Name	Number	Mass (1/Jupiter)	Distance (Jupiter radii)
Io	I	4.7e-05	5.90
Europa	II	2.5e-05	9.39
Ganymede	III	7.8e-05	14.97
Callisto	IV	5.7e-05	26.34

Each of the major moons has a nearly circular equatorial orbit.

For our study, we consider a nominally Europa orbiting trajectory, with initially zero eccentricity,  $60^\circ$  inclination with respect to the Europa orbital plane, and located at about 1.28 Europa radii (2000 km from moon center, about 435 km above its surface). We arbitrarily choose the initial epoch as 1 Jul 2020 12:00:00. The spacecraft can maintain an orbit for just over 70 days before impacting the surface. We compare trajectories over a 30-day span.

First, we compare numerically integrated trajectories using Europa as the reference body. The reference trajectory, for comparison purposes, includes the effects of Europa’s gravity field (a 2x2 field), Jupiter’s gravity field (a 6x0 zonal field), and the third-body point mass effects of the other major moons, the Sun, and the Saturnian, Uranian, and Neptunian systems. All gravitational parameter values and gravity zonals for the celestial bodies are set from values indicated in the comments section of the SPICE files containing the ephemerides, except for Europa’s gravity field which uses the values from Ref. 5. Other celestial bodies in the Jovian system are ignored, as are relativistic effects.

The maximum difference between the trajectories being studied and the reference, for a 30-day propagation, is shown below in Table 8.

**Table 8: Maximum difference against 6x0 Jovian field, using Europa reference frame**

Jupiter’s gravity field	Maximum difference (m)
4x0	0.004
3x0	3.02
2x0	3.03
Point mass	3,370

One should note that while the J3 term is non-zero, it is very small compared to the other zonals and provides little improvement over inclusion of the J2 term. Next we repeat the comparison, using Jupiter as the reference body. The reference trajectory is computed using the same force modeling used for the previous reference trajectory, but computed in the Jupiter-referenced frame. The maximum differences are shown below in Table 9:

**Table 9: Maximum difference against 6x0 Jovian field, using Jupiter reference frame**

Jupiter's gravity field	Maximum difference (m)
4x0	7.52
3x0	428
2x0	441
Point mass	726,000

It is clear that Jupiter's J2 perturbation must be included to compute an accurate orbit. For a Europa-referenced trajectory, higher order Jovian oblateness has little influence on the generated trajectory. For a Jupiter-referenced trajectory, a 4x0 field is likely sufficient to meet accuracy needs.

We next perform a study to determine the effect of the using a 4x0 field vs. a 2x0 field, effectively evaluating the influence of J4 on the resulting ephemerides. Europa-referenced trajectories are generated over a range of initial altitudes, using a 4x0 field and then a 2x0 field. Comparisons are made using 14-day propagation spans. The maximum difference between the trajectories, for each given initial altitude, is plotted in Figure 3. The difference varies quadratically with altitude, up to an altitude of 3 km. At higher altitudes, trajectories become more eccentric, being elongated toward Jupiter. In fact, the trajectory with 3.5 km initial altitude impacts the surface within 1 day past the 14 day span. The difference is always on the order of tens of meters, which may be considered to be of no consequence in many applications.

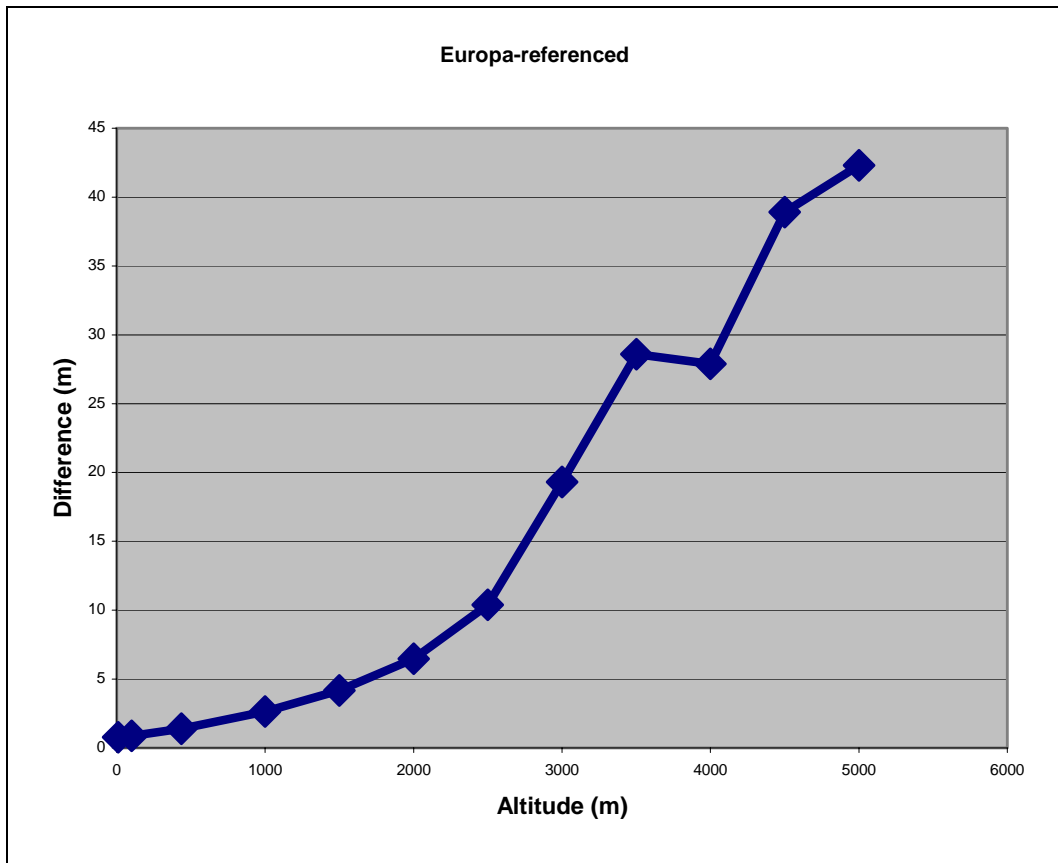


**Figure 3: Position difference between 4x0 and 2x0 Jupiter field, Europa referenced**

We repeat the study using Jupiter-referenced trajectories. Maximum differences are plotted in Figure 4. Again, the difference varies quadratically with altitude, until the altitude is sufficiently large that the trajectory escapes Europa. The magnitude of the difference is on the order of a few kilometers that may be of significant size for certain applications (e.g, mapping).

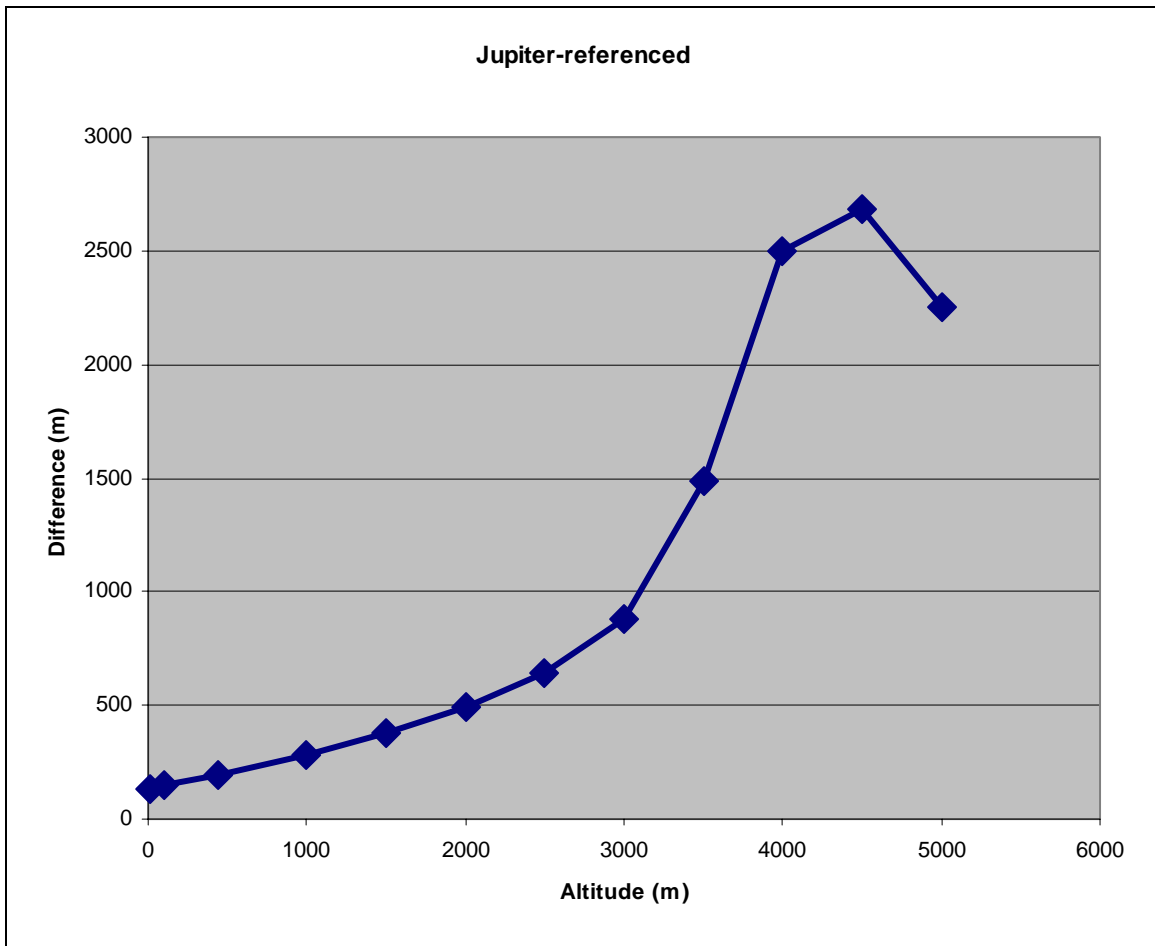


**Figure 4: Position difference between 4x0 and 2x0 Jupiter field, Jupiter referenced**

## SUMMARY

The equations of motion of a spacecraft in an n-body system show that the gravity fields of third-bodies are modeled as tidal effects. In the Earth-Moon system, the field of the Moon does not have a significant effect on Earth-orbiting spacecraft, and the field of the Earth does not have a significant effect on Moon-orbiting spacecraft. The Moon's field also does not have a significant effect when targeting a lunar transfer from Earth orbit. However, it may be required during actual mission operations after the maneuver is performed. When orbiting the moon of a gas giant, the gravity field of the planet should be included, though its field has a smaller effect when the moon being orbited is used as the reference body because the effect is tidal. The studies strongly suggest the use of the closest celestial body as the reference body in the equations of motions, so that uncertainties and mismodeling effects appear in the equations as tidal terms where possible.

## REFERENCES

1. "Correct Modeling of the Indirect Term for Third-Body Perturbations," M. M. Berry and V. T. Coppola, AAS 07-417.
2. "Planetary and lunar ephemeris DE418," W. M. Folkner, et al., IOM 343R-07-005, JPL, 2 Aug 2007. Available at [ftp://naif.jpl.nasa.gov/pub/naif/generic\\_kernels/spk/planets/de418\\_announcement.pdf](ftp://naif.jpl.nasa.gov/pub/naif/generic_kernels/spk/planets/de418_announcement.pdf)
3. JPL SPICE files available at: [ftp://naif.jpl.nasa.gov/pub/naif/generic\\_kernels/spk/](ftp://naif.jpl.nasa.gov/pub/naif/generic_kernels/spk/).
4. "The Gravity Field of the Saturnian System from Satellite Observations and Spacecraft Tracking Data," R. A. Jacobson et al., The Astron. J., 132:2520-2526, Dec 2006.
5. "Europa's Differentiated Internal Structure: Inferences from Four Galileo Encounters," Anderson, J. D., et al., Science 281, 2019-2022, 1998.
6. Lemoine, F.G., et. al. "The Development of the Joint NASA GSFC and NIMA Geopotential Model EGM96". NASA/TP-1998-206861. NASA Goddard Space Flight Center, Greenbelt, MD. July 1998. Available at: <http://cdis.gsfc.nasa.gov/926/egm96/nasatm.html>.
7. "Lunar Prospector Spherical Harmonics and Gravity Models". <http://pds-geosciences.wustl.edu/missions/lunarp/shadr.html>. NASA. Updated Dec 2007.
8. "Solar System Strategic Exploration Plans". <http://solarsystem.nasa.gov/missions/future1.cfm>. NASA. Updated Jan 2008.